

Ξ^- and Ξ^+ baryon production in Au+Au collisions at $\sqrt{s_{\text{NN}}} = 130$ GeV

Javier Castillo^a for the STAR collaboration*

^aSUBATECH, Nantes, France

We report preliminary results on the centrality dependence of the Ξ^- and Ξ^+ production at mid-rapidity in $\sqrt{s_{\text{NN}}} = 130$ GeV Au+Au collisions from the STAR experiment. For the most central data the obtained yields suggest a saturation of strangeness production per produced hadron. The calculated inverse slope parameter may indicate an earlier freeze-out of these particles.

1. Introduction

The study of multi-strange baryons in ultra-relativistic heavy ion collisions was first motivated by the prediction of an enhancement of strange $q\bar{q}$ pair production due to the formation of a quark gluon plasma (QGP) compared to that found from a hadron gas state [1]. The enhancement is thought to be more pronounced for multi-strange baryons and anti-baryons since their production is strongly suppressed in hadronic interactions due to their high mass thresholds [2]. Also, by comparing the multi-strange baryon yields and ratios to other particles with those predicted from particle production models, one can test whether the system has reached chemical equilibrium or not. The study of transverse momentum spectra will allow us to test the thermal equilibration of the system.

The Relativistic Heavy Ion Collider (RHIC) allows for the study of nuclear matter in extreme conditions such as in the case of the theoretical QGP. We present here preliminary measurements of multi-strange baryon production at mid-rapidity as a function of the collision centrality in $\sqrt{s_{\text{NN}}} = 130$ GeV Au+Au collisions from the STAR experiment.

2. Experimental setup and data analysis

The data presented here were taken with the STAR detector during the year 2000 Au+Au at $\sqrt{s_{\text{NN}}} = 130$ GeV run. The experimental setup for this period consisted mainly of a large cylindrical Time Projection Chamber (TPC) used for charged particle tracking and identification. A Central Trigger Barrel (CTB) and two Zero Degree Calorimeters (ZDC) were used for triggering. More details of the experimental setup can be found in [3]. The data were divided into three centrality classes corresponding to 0–10%, 10–25% and 25–75% of the total hadronic cross section as described in [4].

The multi-strange Ξ^- particles were reconstructed via their decay topologies, $\Xi^- \rightarrow \Lambda\pi^-$ followed by $\Lambda \rightarrow p\pi^-$ with a branching ratio of 100% and 64% respectively. The reconstruction of Ξ^- particles was handled by first reconstructing Λ candidates as described

*For the full author list and acknowledgments, see Appendix “Collaborations” of this volume.

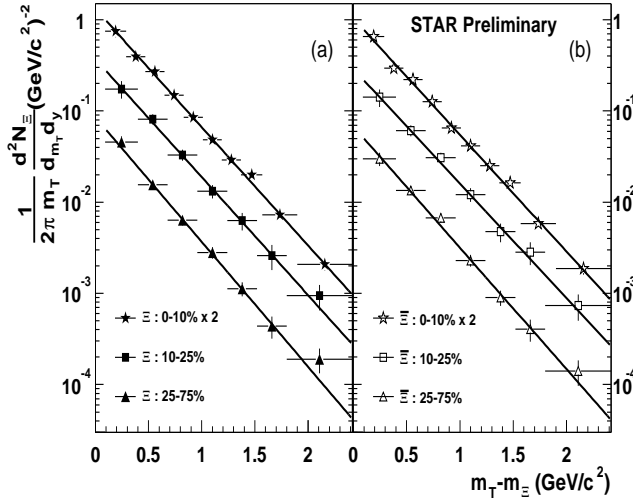


Figure 1. Transverse mass spectra of (a) Ξ^- and (b) Ξ^+ as a function of collision centrality. Lines are exponential fits to the data.

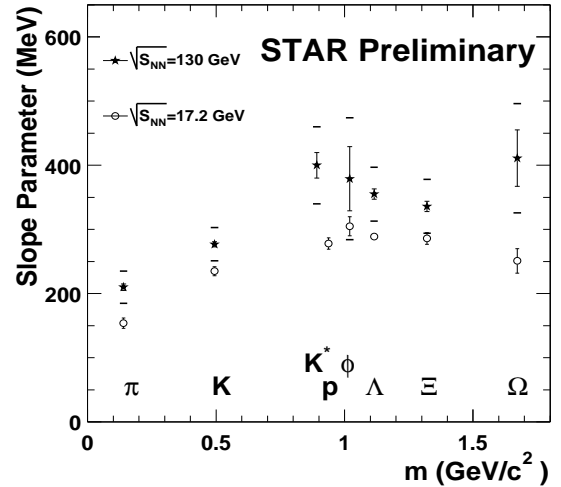


Figure 2. Inverse slope parameter as a function of particle mass for (circles) SPS and (stars) RHIC central collisions.

in [3]. These Λ candidates were then extrapolated backwards and combined with negatively charged tracks to determine Ξ^- candidates, and similarly for the charge conjugate Ξ^+ decay. Particle identification from energy loss of charged tracks in the TPC as well as simple geometric and kinematic cuts were applied at both steps to reduce the large combinatorial background inherent to such a reconstruction process. For Ξ^- and Ξ^+ the raw yields were extracted from the invariant mass distribution by counting the entries within ± 15 MeV/ c^2 about the expected mass and then subtracting the background. The background under the peak was estimated by sampling two regions on either side.

3. Results and Discussion

The invariant mass distribution of Ξ^- (Ξ^+) candidates was then histogrammed in transverse mass $m_T = \sqrt{p_T^2 + m_0^2}$ bins and the signal extracted in each bin as described above. Each m_T bin was then corrected for detector acceptance and reconstruction efficiency by the Monte Carlo technique where simulated Ξ^- particles were embedded into real events. The data cover $|y| < 0.75$, simulations showed that the acceptance and efficiency for Ξ is constant, in y , over this range.

3.1. Centrality dependence of invariant yields and slope parameter

Each of the obtained preliminary m_T spectra for Ξ^- and Ξ^+ for the three centrality classes used in this analysis was then fit to an exponential function ($\propto \frac{dN}{dy} e^{-(m_T - m_0)/T}$) to determine simultaneously the inverse slope, T , and the rapidity density, $\frac{dN}{dy}$, integrated over all m_T . The results are summarized in table 1. We observe that the slope parameter is, within error bars, the same for Ξ^- and Ξ^+ and is not strongly dependent on centrality. Also the $\frac{dN}{dy}$ for Ξ^- and Ξ^+ is found to increase linearly with $dN_{h-}/d\eta$. Thus, no noticeable

	Centrality	0 – 10%	10 – 25%	25 – 75%
Ξ^-	dN/dy	2.30 ± 0.09	1.29 ± 0.12	0.28 ± 0.02
	T (MeV)	335 ± 6	336 ± 18	318 ± 14
Ξ^+	dN/dy	1.89 ± 0.08	1.08 ± 0.11	0.24 ± 0.2
	T (MeV)	338 ± 7	344 ± 18	325 ± 14

Table 1

Mid-rapidity fit parameters from exponential fit to Ξ^- and Ξ^+ m_T spectra.

change of the production mechanism for Ξ baryons is observed in the covered centrality region. Systematic errors are estimated to be $\sim 20\%$. The feeddown from weak decay of $\Omega^-(\bar{\Omega}^+)$ on $\Xi^-(\bar{\Xi}^+)$ is estimated to be less than 2% and thus it has been neglected for this analysis. The Ξ^- and Ξ^+ particle yields in the measured m_T region correspond to $\sim 75\%$ of the total yield.

3.2. Systematics of the inverse slope parameter

Figure 2 shows the mid-rapidity inverse slope parameters as a function of particle mass, for central Pb+Pb collisions at $\sqrt{s_{NN}}=17.2$ GeV [5,6,7] and preliminary results from Au+Au collisions at $\sqrt{s_{NN}}=130$ GeV [3,8,9,10]. Note that both, statistical errors and systematic errors (horizontal lines) are reported on STAR points, while SPS points only include statistical errors. We observe the following : the inverse slope parameters are higher in RHIC collisions than in SPS collisions and the strange baryons seem to deviate from the collective flow pattern driven by lighter particles at both energies. The relatively low inverse slope parameter found for the Ξ baryons may be due to the functional form and the m_T range used for the fit or it could indicate, as proposed in [12], that they freeze-out earlier during the system's evolution.

3.3. Non-identical particle ratios

Figure 3 shows the mid-rapidity ratios (a) Ξ/h^- and (b) Ξ/Λ from heavy ion collisions at SPS [11], plus preliminary RHIC results. The $\bar{\Xi}^+/h^-$ ratio increases with beam energy indicating a higher excitation energy from the collision reached at RHIC energies compared to SPS energies. On the other hand, the Ξ^-/h^- ratio remains constant from SPS to RHIC energies due to the competing effect of the dropping net-baryon density. Also from SPS to RHIC energies, the Ξ^-/Λ ratio increases due again to the drop of the net-baryon density which causes a smaller fractional rise on Λ than on Ξ^- , while the $\bar{\Xi}^+/\bar{\Lambda}$ is constant. The behaviour of $\bar{\Xi}^+/\bar{\Lambda}$ suggests a saturation of the strangeness production from SPS to RHIC. Note that Ξ^-/Λ and $\bar{\Xi}^+/\bar{\Lambda}$ ratios have been corrected for feeddown from weak decays of Ξ on Λ . For SPS values the quoted [5] upper limits of 5% for Λ and 10% for $\bar{\Lambda}$ were used.

Particle ratios between dissimilar species can be used to test particle production models. Using preliminary STAR data we have obtained $\Xi^-/\pi^- = 0.0088 \pm 0.0004$. ALCOR, a quark coalescence model, overestimates the Ξ^-/π^- ratio by almost a factor of two [13]. A statistical model assuming local chemical equilibrium and strangeness neutrality [14] is, within systematic errors, in agreement with the experimental value of Ξ^-/π^- ratio. Finally the authors of [15] need to assume chemical non-equilibrium in their QGP model to better address the Ξ^-/Λ ratio.

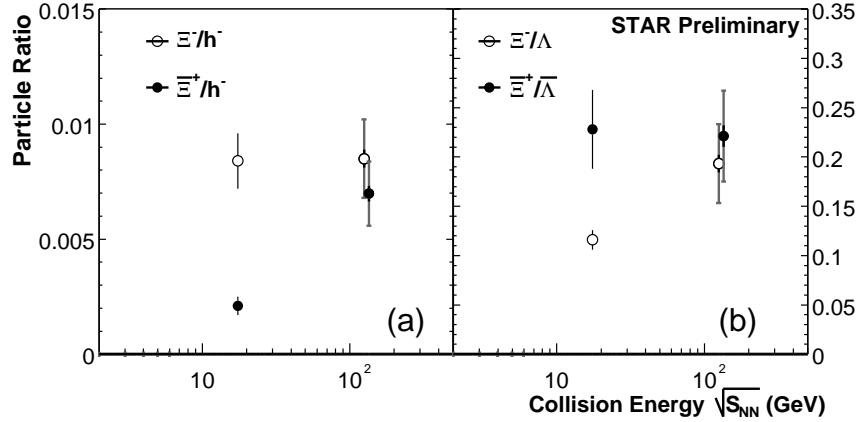


Figure 3. Mid-rapidity (a) Ξ^-/h^- ratios and (b) Ξ^-/Λ ratios as a function of beam energy. Systematic errors to STAR points are shown in gray.

4. Conclusion

In summary, the Ξ^- and Ξ^+ invariant yields at mid rapidity increase linearly with the number of produced negative hadrons. The production of strangeness per produced hadron seems to saturate from SPS to RHIC energies, which is consistent with the system being in chemical equilibrium. The extracted inverse slope parameters are the same for both Ξ^- and Ξ^+ and are not strongly dependent with centrality. For central collisions this inverse slope parameter is higher than that from collisions at the SPS energy and shows a deviation from a collective flow pattern that may indicate an earlier freeze-out of multi-strange baryons.

REFERENCES

1. B. Müller and J. Rafelski, Phys. Rev. Lett. **48** (1982) 1066.
2. J. Rafelski, Phys. Lett. **B262** (1991) 333.
3. C. Adler *et al.* (STAR Collaboration), Phys. Rev. Lett. **89**, 092301 (2002)
4. K.H. Ackermann *et al.* (STAR Collaboration), Phys. Rev. Lett. **86** (2001) 402.
5. F. Antinori *et al.* (WA97 Collaboration), Eur. Phys. J. **C14** (2000) 633-641.
6. I.G. Bearden *et al.* (NA44 Collaboration), Phys. Rev. Lett. **78**, (1997) 2080.
7. S. V. Afanasev *et al.* (NA49 Collaboration), Phys. Lett. **B491** (2000) 59.
8. J. Harris *et al.* (STAR Collaboration), Nucl. Phys. **A698** (2002) 64c-77c.
9. C. Adler *et al.* (STAR collaboration) Phys. Rev. C **65**, 041901(R) (2002)
10. C. Suire for the STAR collaboration, these proceedings.
11. F. Antinori *et al.* (WA97 Collaboration), Nucl. Phys. **A661** (1999) 130c.-139c.
12. H. van Hecke, H. Sorge and N. Xu, Phys. Rev. Lett. **81**, 5764 (1998)
13. T. Biró, P. Lévai, and J. Zimányi, J. Phys. G **28**, 1561 (2002)
14. P. Braun-Munzinger *et al.*, Phys. Lett. **B518**, 41(2001).
15. J. Rafelski and J. Letessier, arXiv:hep-ph/0206145